Design of the TM₀₁₀ mode cylindrical cavity resonator for PCB dielectric characterization

Reza Asadi EMC Laboratory Missouri University of Science and Technology Rolla, USA reza.asadi@mst.edu Chaofeng Li
EMC Laboratory
Missouri University of Science and
Technology
Rolla, USA
clf83@mst.edu

Seyedmehdi Mousavi EMC Laboratory Missouri University of Science and Technology Rolla, USA smousavi@mst.edu

Seyed Moastafa Mousavi EMC Laboratory Missouri University of Science and Technology Rolla, USA seyedmostafa.mousavi@m st.edu Reza Vahdani EMC Laboratory Missouri University of Science and Technology Rolla, USA r.vahdani@mst.edu Xiaoning Ye
Data Center and AI Group
Intel Corporation
Jones Farm, USA
xiaoning.ye@intel.com

DongHyun (Bill) Kim EMC Laboratory Missouri University of Science and Technology Rolla, USA dkim@mst.edu

This paper presents the study of the TM₀₁₀ mode cylindrical resonator, which can be used for printed circuit board (PCB) material properties extraction, e.g., the dielectric constant (Dk) and the loss tangent (Df) extraction. The theoretical formulas of the resonance frequency and O-factor of the resonator are presented. In real measurement, the TM₀₁₀ mode cylindrical cavity resonator needs to be excited by the probe. The study emphasizes the impact of probe orientation, location, and field distribution on the accuracy of material property extraction. The relationship between cavity dimensions and resonance frequency is explored, highlighting the influence of cavity radius and height on material property characterization. Visual representations and simulations illustrate the significance of these dimensions in accurately determining Dk and Df. The paper also compares the efficiency of electric- (E-) and magnetic- (H-) probe feeding methods through full-wave simulations. Results indicate that the E probe exhibits superior accuracy, with relative errors below 0.2% for Dk and less than 2.2% for Df, while the H probe shows a relative error of 0.1% for Dk and 8% for Df. The presented analysis can help the development and the manufacture of the cavity resonator method, for characterizing the PCB material.

Keywords—PCB material characterization, Electric probe, Magnetic probe, cavity feeding, Dk, Df, cavity resonator, TM_{010} mode.

I. INTRODUCTION

Nowadays, the dielectric material plays a crucial role in various printed circuit board applications, e.g. antenna and filter design, system-on-chip development, and system-inpackage implementation [1, 2]. Besides, the PCB dielectric material could cause a critical signal integrity issue for the high-speed applications [3], such as loss and crosstalk [4, 5]. It would be very helpful for the PCB design if the PCB material can be accurately characterized. Numerous techniques have been developed for the characterization of PCB dielectric materials, falling into two main categories: non-resonant and resonant methods. Non-resonant methods encompass a variety of approaches, such as the transmission line-based method [6], coaxial probe method [7], parallel plate method [8-10], and free space method [11]. These techniques are capable of characterizing materials across a broad bandwidth, particularly effective for analyzing lossy materials. On the other hand, resonant methods, including the cavity resonator method [12] and resonator sensor [13], These

methods are used to extract the dielectric constant (Dk) and loss tangent (Df) of the PCB dielectric at a specific resonance frequency. Accurately determining a material's Dk and Df is crucial for various applications, and the cylindrical cavity resonator has long been recognized as a reliable method for this purpose. This method operates across different frequency ranges, depending on the resonator's dimensions. The cavity resonator can work in different modes, such as transverse electric (TE) mode or transverse magnetic (TM) mode. The electric field distribution in the cavity resonator varies with the mode. Due to the inhomogeneity of the PCB dielectric, the Dk and Df values extracted by different methods may differ. For PCB applications, the TM mode resonator is preferable because the electric fields in a TM mode resonator are similar to the electric field distribution in a transmission line.

This paper focuses on the theoretical calculation of the TM_{010} resonance frequency and explores the impact of the probe on extracting Dk and Df of PCB substrate martial in the real measurement. The calculations specifically address the ideal mode, requiring external excitations for TM_{010} realization, which can be achieved through electric (E probe) and magnetic (H probe) probes. In the second part of this paper, E and H probes are compared as two different feeding methods for cavity resonators. The discussion delves into probe orientation, probe location, and fields distribution analysis for both methods. Finally, the efficiency of E probe and H probe feeding methods is compared through full wave simulation to find the impact of probes on material extraction results.

II. TM₀₁₀ MODE CYLINDRICAL CAVITY RESONATOR

The resonator dimension and the dielectric material in the cavity determine the resonance of the cylindrical cavity resonator. The resonance frequencies of TM mode cylindrical cavity resonator can be calculated individually using equation (1), as described in [14]. These calculated frequencies provide valuable insights into the dynamics of the cavity resonators and contribute to the overall understanding of their operational characteristics. The dependence of resonances on the cavity size and dielectric properties highlights the significance of accurate characterization and control of these parameters in the design and optimization of cylindrical cavity resonator-based systems.

$$f_{c_{TMnml}} = \frac{C}{2\pi\sqrt{\mu_{r}\varepsilon_{r}}} \sqrt{\left(\frac{P_{nm}}{a}\right)^{2} + \left(\frac{l\pi}{d}\right)^{2}}$$
(1)

Here, c denotes the wave velocity in free space, while μ_r represents the magnetic constant or permeability, and ε_r refers to the dielectric permittivity. The variables 'a' and 'a' represent the radius and height of the cavity respectively. Moreover, the terms P'_{nm} and P_{nm} symbolize the ordered zeros of J'0(x) and $J_0(x)$ correspondingly. where the indices. m, n, l indicate the number of variations in the standing wave pattern in the r, ϕ and z directions.

Another parameter that should be calculated in a cavity resonator is the Q factor, which quantifies the stored energy at the resonance frequency and is used to calculate the material's loss. In this paper, we analyzed the TM_{010} mode cylindrical cavity resonator for PCB dielectric Dk and Df characterization. Fig. 1 shows electrical (E) and magnetic (H) fields in the cylindrical cavity works at TM_{010} mode. It shows that E field direction is vertically distributed while H filed is horizontally distributed in ϕ direction.

The TM_{010} mode resonance frequency of a cylindrical cavity resonator can be calculated based on the cavity radius and the material property inside the cavity, as shown in (1).

$$f_{TM010} = \frac{C}{2\pi\sqrt{\varepsilon_r}} \times \frac{P_{01}}{a} \tag{2}$$

Where c denotes the wave velocity in free space, and ε_r refers to the dielectric permittivity. The variable a represents the radius t of the cavity. moreover $P_{01} = 2.404$.

The Q-factor of the cylindrical cavity resonator can also be calculated by the equation (3-a) [15]. The cavity Q-factor related to the conductor loss of the cavity conduct and the loss caused by the material inside the cavity, as shown in equation (4-a).

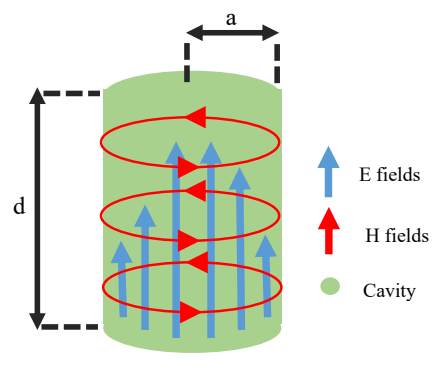


Fig. 1. Schematic representation of electric and magnetic waves in TM mode inside a cylindrical cavity.

The Q_{material} represents the Q-factor related to the material loss while the Qc denotes the Q-factor when the cavity is empty, these equations are used for real calculation.

$$Q_{010}^{TM} = \left(\frac{P_{01}\eta}{2R_s\left(1 + \frac{a}{d}\right)}\right)$$
 [15] (3-a)

$$R_s = \sqrt{\mu_0 \pi f_{010}^{TM} / \sigma}$$
 [15] (3-b)

$$\frac{1}{Q_{calculated}} = \frac{1}{Q_{material}} + \frac{1}{Q_c}$$
 [15] (4-a)

$$\frac{1}{Q_{material}} = tan\delta$$
 [15] (4-b)

In equations (3-a) and (3-b), μ represent the permittivity and permeability of air, respectively. Rs denotes the surface resistance of the cavity conductor, while d represents the height of the cavity. The symbol σ stands for the conductivity of the cavity conductor, and $tan\delta = 1/Q_{material}$ signifies the dissipation factor (Df) of the material enclosed within the cavity.

In Figure 2, we show how the radius of the cavity affects the resonance frequency of the TM_{010} mode when the cavity is filled with a material that has a dielectric constant (Dk) of either 1 or 2. As you can see, the resonance frequency drops as the cavity radius gets larger. This means we can control the resonance frequency by adjusting the cavity radius. When the cavity is filled with a material that has a higher Dk than air, the resonance frequency decreases. By observing this frequency change, we can determine the Dk of the material. For example, Figure 2 illustrates that for a material with a Dk of 2, the cavity radius should be about 5.7 mm at 14 GHz, 11.5 mm at 7 GHz, and 110 mm at 1 GH.

In addition to determining the radius of the cavity, another crucial dimension to determined is the height of the cavity. This can be accomplished by utilizing equations (3-a) and (3-b), as explained in the analytical framework. In real measurement, the Q-factor of the resonator can be measured by the instrument depends on the accuracy of the

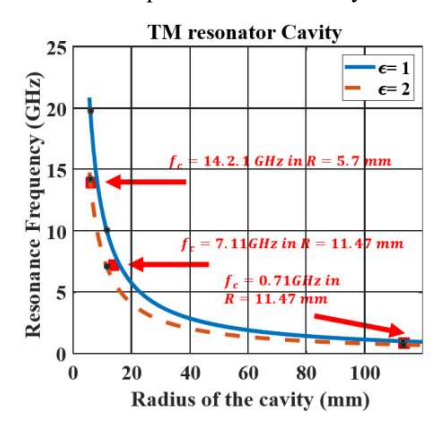


Fig. 2. TM_{010} resonance frequency across dimensional ranges for materials with DK values of 2 and 1

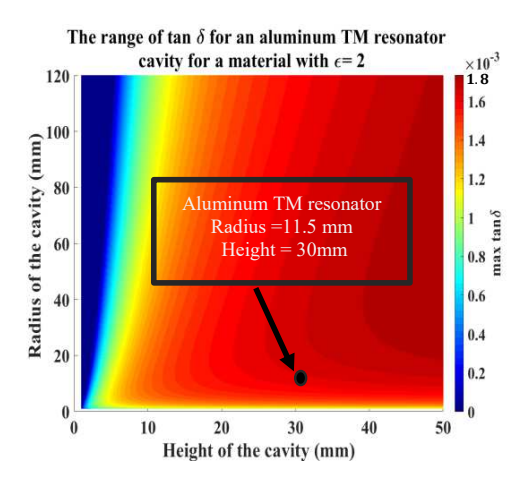


Fig. 3. Effect of cavity dimensions on the maximum value of Df that can be measured in this method

measurement process. But the Q-factor value of the resonator would impact the accuracy of the measurement. In other words, the Q-factor of the resonator at the working mode cannot be too minimum, which cannot be accurately measured. If assumed the minimum value of the Q factor that can be measured is around 90, the maximum value of the DF in the cavity resonator can be calculated. Fig 3 provides visual insights, depicting the maximum value of Df that can be calculated within a cavity measuring 11.5 mm by 30 mm, measurable a calculated value of 1.6×10^{-3} . This information underscores the significance of considering cavity height in relation to the material loss tangent for accurate calculation.

III. TM_{010} mode feeding

This paper explored the impact of the probe used to feed the cylindrical cavity resonator. A complete analysis and the probe manufacturing challenges were conducted. In practical applications, the cylindrical cavity should be feeded by the probe. The pursuit of this goal requires an investigation into two different feeding options: the H probe and E probe methods. This section delves into these feeding techniques, emphasizing their importance in the context of the study and providing insights into the challenges encountered during the manufacturing process.

A. Resonator with H-probe

The loop antenna can be regarded as an H probe, receiving magnetic fields in a manner akin to a human hand. Fig 4 presents a diagram of the loop, designed for utilization in TM resonators. These probes possess a current loop that emits a magnetic field, with the orientation of this field crucially dependent on the right-hand rule, where the H field is perpendicular to the current direction. As depicted in Fig 1, in TM mode, the H direction aligns with the $\hat{\phi}$ direction, corresponding to the current's \hat{z} direction.

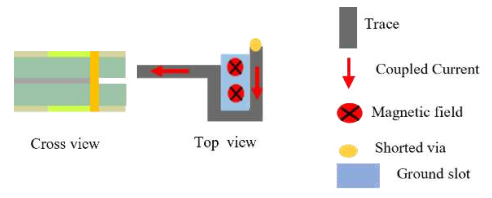


Fig. 4. Schematic of H probe (loop) mechanism

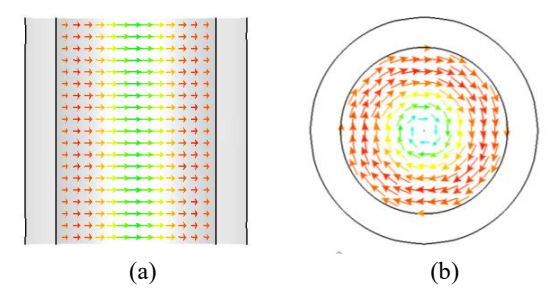


Fig. 5. Simulation results of the magnetic field direction within a cylindrical cavity in TM_{010} mode. (a) Side view. (b) Top view.

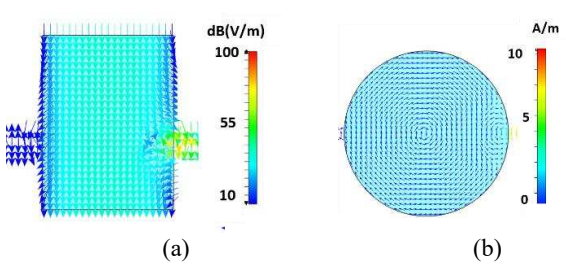


Fig. 6. Full-wave simulation results of electric and magnetic field directions within a cylindrical cavity fed by an H probe (loop) in TM_{010} mode. (a) Side view of electric field direction. (b) Top view of magnetic field direction

As depicted in Fig 5 which is results of eigenmode simulation, the magnetic fields exhibit increased strength near the walls of the cavity, maintaining a consistent intensity at various heights. When placing the H probe, it is advisable to place two holes within the cavity, positioned far from the upper and lower extremities, to mitigate potential effete of top and bottom walls. Placing these holes as far away as possible from the upper and lower metallic components is vital, making the middle height the strategically preferred location for the feeding holes in the H probe setup.

The illustration in Fig 5 (a) and (b) depicts the orientation of magnetic and electric fields within a cavity influenced by a H field loop probe. Through full wave simulations and eigenmode analysis, it is revealed that the TM_{010} mode is generated within this cavity, and the H probe has the capability to feed this mode.

B. Resonator with E-probe

An alternative method for energizing the transverse magnetic (TM) mode within a cylindrical cavity involves utilizing an E probe as the feeding mechanism. the coaxial feeding is able to realize E probe to fed TM mode. The optimal placement of the E probe within the cavity can be determined with the assistance of Fig 7. In Fig 7, a top view of the E field density is presented, offering insights into the most favorable location for the E probe. Based on this analysis, the ideal position for the E probe is identified as the center of the cavity, both at the top and bottom.

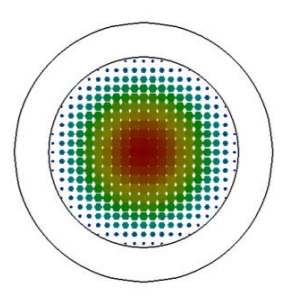


Fig. 7. Result of eigenmode simulation in cavity that shows electric fields direction in TM_{010}

Fig 8 a and b illustrates side and top view of schematic of resonator which is fed by E probe. These pictures show the expected magnetic and electric filed which have been validated through full-wave simulation. The simulation results are presented in Figures 9a and 9b. In Figure 9a, the side view of the cavity displays the electric field direction aligned with the \widehat{Z} direction. In Figure 9b, the top view reveals the magnetic field direction consistent with the $\widehat{\phi}$ direction.

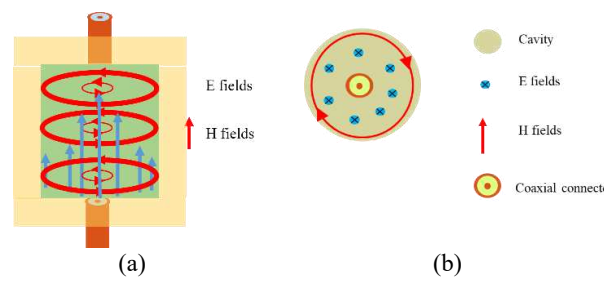


Fig. 8. Schematic of E probe mechanism and field drection view. (a) side view, (b) Top view

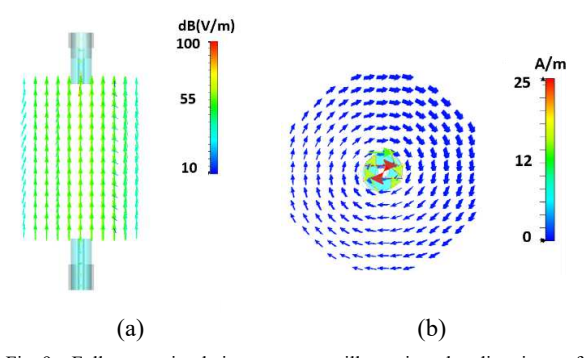


Fig. 9. Full-wave simulation outcomes illustrating the directions of electric and magnetic fields within a cylindrical cavity fed by an E probe in TM_{010} mode. (a) Electric field direction in side view. (b) Magnetic field direction in top view.

IV. RESULTS AND DISCUSSION

As previously discussed, the calculation of a material's Dk and DF is facilitated by this method. In this paper, an attempt is made to compare two approaches for feeding the TM mode of a cylindrical cavity, aiming to determine which method is suitable for calculating the material parameters of high-loss materials.

In the preceding section, it was determined that the TM mode within the cylindrical cavity can be facilitated by both the E probe and H probe. The subsequent section explores the effects of different probes on the results of material extraction. The simulated cavity dimensions consist of an 11.3 mm radius and a 30 mm height. Another factor we need to consider is how well metal conducts electricity. We chose aluminum because it gives us accurate results.

For calculating Dk and Df using equations (2) and (3), such as the probe factor, aluminum conductivity, and dimensional changes in different atmospheres, remain unknown. To address this, a calibration step becomes necessary, and it can be determined by measuring the resonance frequency and Q factor of a known material, like Air. The accurate cavity radius can be determined using the resonance frequency of an empty cavity and equation (2). It is important to highlight the calculation of Q_c which incorporates the effects of aluminum conductivity and the probe factor on the Q factor. This parameter is computed using equation (3-a), and the results serve as a correction factor applicable in Dk calculations.

As the next step, the dielectric constant (Dk) of the material under test (MUT) can be determined by measuring its resonant frequency and applying equation 3. Subsequently, MUT's loss tangent (Df) is calculated using the known parameters with equation 4. The simulation results presented in the following demonstrate the impact of the feeding method.

The validation of this method is conducted through a full-wave simulation, as illustrated in Figure 10, which compares the impacts of the E probe and H probe within an empty cavity. It is observed that the resonance peak level with the E probe is 25 dB higher than that with the H probe, with respective Q factors of 1693 and 3900. The Q factor of the response involves factors such as material loss, conductivity, and the Q factor of the probe. In an empty cavity, the dominance of the probe's Q factor results in a higher Q factor for the S21 resonance in the H probe. The higher peak observed in the E probe is attributed to its location within the maximum electric field, enabling it to achieve a better peak compared to the H probe.

In Figure 11, a comparison is made among cavities with different feeding mechanisms, all fully filled with materials possessing the same Dk value of 2 but varying Df values. The aim is to assess the impact of the loss tangent on the results.

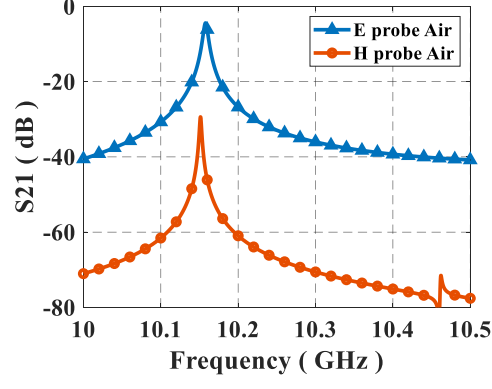


Fig. 10. Comparison of resonance peaks between two different cavity feeding methods: E probe and H probe, both in the empty case

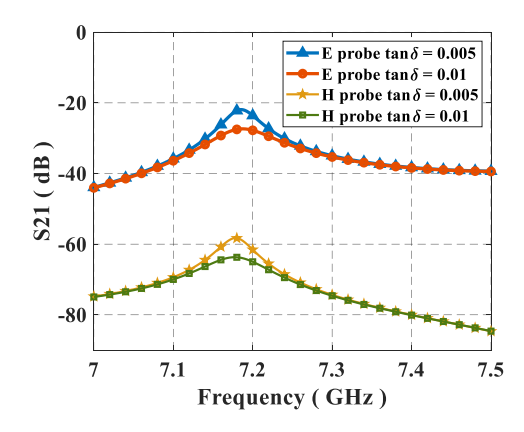


Fig. 11. Effect of feeding probe on resonance peak in a fully filled cavity with materials having the same Dk (=2) but varying Df (0, 0.005, and 0.01).

TABLE I. DK AND DF EXTRACTED BY SIMULATION IN TWO E AND H FEEDING METHODS

Probes type	DF	Fc (GHz)	Q factor	Peak (dB)	DK _{Cal}	Df _{CAl}
E probe	5×10 ⁻³	7.18	171	-22	1.99	5.1×10 ⁻³
	10×10 ⁻³	7.19	91	-27	1.99	10.2×10 ⁻³
H probe	0.005	7.178	174	-58	2	5.4×10 ⁻³
	0.01	7.17	91.5	-63	2.002	10.6×10 ⁻³

Simulations for Dk values of 0.005, and 0.01 are conducted, and a detailed comparison is presented in Table 1. The calculation of Dk and Df is based on the simulation, revealing that the relative errors in Dk and Df extraction through the E probe are below 0.2% for Dk and less than 2.2% for Df in cases of low loss. In the case of the H probe, relative errors are approximately 0.1% for Dk and 8% for Df.

Resonance peak level is another important parameter to investigate in this simulation. E probe peaks 36 dB higher than H probe method in average. This difference helps to detect resonance in high loss material and allow to use VNA as a measurement equipment in low power input.

V. CONCLUSION

In this paper, we introduced a method to figure out the properties of PCB material, specifically its Dk (dielectric constant) and Df (dissipation factor). We used a cylindrical cavity resonator for this and explored how the size of the cavity affects the measurements. We discovered that the height of the cavity influences the extraction of Df, and for high Df, a shorter cavity works better. We showed that both E probe and H probe feeding can be used in the cylindrical cavity resonator to accurately find Dk and Df. When we tested the same material using both probes, we found that the Q factor and resonance frequency were almost identical. For instance, the extracted Q factor with an E probe for a material

with Dk 5×10-3 was 171, and with an H probe, it was 174. When calculating Dk and Df, the relative errors using the E probe were less than 0.2% and 2.2%, respectively. However, when using the H probe, the relative error for Df was higher at 8%, even though the error for Dk was only 0.1%. One notable difference between the two methods is the resonance peak value, with the E probe showing a peak 35 dB higher than the H probe. This higher peak detection ability of the E probe is useful for identifying resonances in materials with high loss. In the next phase, we plan to validate these methods through measurements to evaluate how well they actually perform.

REFERENCES

[7]

- [1] C.-Y. Ho, H.-H. Cheng, P.-C. Pan, C.-C. Wang, and C.-P. Hung, "Dielectric characterization of ultra-thin low-loss build-up substrate for system-in-package (SiP) modules," *IEEE Transactions on Microwave Theory and Techniques*, vol. 63, no. 9, pp. 2923-2930, 2015.
- [2] N. K. Tiwari, S. P. Singh, A. K. Jha, and M. J. Akhtar, "Simplified approach for broadband RF testing of low loss magneto-dielectric samples," *IEEE Transactions on Instrumentation and Measurement*, vol. 69, no. 5, pp. 2248-2257, 2019.
- [3] Y. Liu et al., "Inhomogeneous Dielectric Induced Skew Modeling of Twinax Cables," *IEEE Transactions on Signal and Power Integrity*, 2023.
- [4] Y. Liu et al., "An Empirical Modeling of Far-End Crosstalk and Insertion Loss in Microstrip Lines," *IEEE Transactions on Signal* and Power Integrity, vol. 1, pp. 130-139, 2022.
- [5] Y. Liu et al., "Far-End Crosstalk Modeling and Prediction for Stripline With Inhomogeneous Dielectric Layers (IDLs)," IEEE Transactions on Signal and Power Integrity, vol. 1, pp. 93-103, 2022
- [6] J. Mateu, N. Orloff, M. Rinehart, and J. C. Booth, "Broadband permittivity of liquids extracted from transmission line measurements of microfluidic channels," in 2007 IEEE/MTT-S International Microwave Symposium, 2007, pp. 523-526: IEEE.
 - A. Mirbeik-Sabzevari and N. Tavassolian, "Characterization and validation of the slim-form open-ended coaxial probe for the dielectric characterization of biological tissues at millimeter-wave frequencies," *IEEE Microwave and Wireless Components Letters*, vol. 28, no. 1, pp. 85-87, 2017.

 M. T. Khan and S. M. Ali, "A brief review of measuring
- [8] M. T. Khan and S. M. Ali, "A brief review of measuring techniques for characterization of dielectric materials," *International Journal of Information Technology and Electrical Engineering*, vol. 1, no. 1, pp. 1-5, 2012.
- [9] S. Afshar, F. Nazari, and H. Aliakbarian, "A modified methodology for dielectric constant measurement of an arbitraryshaped sheet by using capacitance technique," *European Journal* of *Physics*, vol. 42, no. 3, p. 035205, 2021.
- [10] H. Manoharan, R. He, F. Ma, D. Beetner, B. Booth, and K. Martin, "Influence of Conformal Coatings on the EMC Performance of a Printed Circuit Board," in 2022 Asia-Pacific International Symposium on Electromagnetic Compatibility (APEMC), 2022, pp. 605-607: IEEE.
- [11] J. Krupka, "Frequency domain complex permittivity measurements at microwave frequencies," *Measurement Science* and Technology, vol. 17, no. 6, p. R55, 2006.
- [12] Z. Li, Z. Meng, F. Fei, and A. Gibson, "Microwave Cylindrical Cavity Resonator Sensor for Detection and Characterization of Contaminants in Lubricating Oil," *IEEE Sensors Journal*, vol. 22, no. 23, pp. 22600-22609, 2022.
- [13] L. V. H. Sepulveda, J. L. O. Cervantes, and C. E. Saavedra, "Multifrequency coupled-resonator sensor for dielectric characterization of liquids," *IEEE Transactions on Instrumentation and Measurement*, vol. 70, pp. 1-7, 2021.
- [14] D. M. Pozar, Microwave engineering. John wiley & sons, 2011.
- [15] R. F. Harrington, *Time-harmonic electromagnetic fields*. 2001.